High Energy Electron–Proton Physics at HERA

H1 COLLABORATION PROPOSAL 750

The Universities of Birmingham, Lancaster, Liverpool, Manchester, Queen Mary and Westfield College, University of London and Rutherford Appleton Laboratory

with

RWTH Aachen (I and III Inst.), Universities of Brussels, Cracow, Dortmund, JINR Dubna, CEA Saclay, DESY–Hamburg, DESY–Zeuthen, Universities of Hamburg (II Inst.), Heidelberg, MPI Heidelberg, Universities of Kiel, Kosice, Lund, CPPM-Marseille, ITEP Moscow, LPI Moscow, MPI Munich, LAL Orsay, Ecole Polytechnique, Universities of Paris VI, Paris VII, Prague, Rome, PSI-Villigen, University of Wuppertal, Yerevan Physics Institute, ETH Zürich and University of Zürich

1 Introduction and Overview

The electron-proton collider, HERA performed well during 1999, whilst the H1 experiment took data with high efficiency. Between January and April, 14.2 pb^{-1} of e^-p data were collected. A shutdown of two months then took place to enable the accelerator and experiments to carry out essential maintenence and upgrade work. From July until December, the accelerator ran successfully in e^+p mode. A luminosity of 20.9 pb^{-1} was collected by H1 under normal running conditions. A further sample of 4.6 pb^{-1} was taken with minimum bias triggers, which will enable precision measurements in the low parton-x region. The large integrated luminosities will allow the experiment to carry out its full planned programme prior to the major upgrade of the HERA collider [1], to take place from September 2000. There will then be a shutdown of nine months, during which focusing magnets will be inserted in and around H1. The HERA upgrade is expected to yield a factor of five in luminosity delivered. Several components of H1 will be upgraded at the same time.

The UK groups have been heavily involved in many H1 activities in the past year, making leading contributions to detector operation, physics analysis and upgrade preparations. Sections 2, 3 and 4 of this report contain short descriptions of these activities. Sections 6, 7, 8, and 9 document the publications, conference and workshop contributions and Ph.D. theses that have been produced as a result

2 Physics Results

There have been a number of notable new results from the experiment in 1999, with a strong UK involvement in many cases. A summary of analysis work from the past year involving UK physicists is given below.

2.1 Deep–Inelastic Scattering at Very High Q^2

Inclusive Deep-Inelastic Scattering (DIS) cross-sections have long been used as sensitive probes of proton structure and QCD dynamics. The large integrated luminosity collected with both lepton charges in the colliding ep beams of the HERA accelerator have allowed the phase space of such measurements to be extended into new kinematic regions of very high Q^2, up to 30 000 GeV^2. In this region where $Q^2 \simeq M_Z^2$ or M_W^2, the Z^0 and $W^\pm$ boson masses squared, the electroweak sector of the Standard Model (SM) can be tested in DIS. In addition, signals of new physics beyond the Standard Model may be expected to arise at the highest Q^2 where the smallest distance scales of proton structure are probed.

The neutral current (NC) cross-section for the process $e^\pm p \to e^\pm X$ with unpolarised beams is given by

$$\frac{\mathrm{d}^2\sigma^\pm_{NC}}{\mathrm{d}x\,\mathrm{d}Q^2} = \frac{2\pi\alpha^2}{xQ^4}\left[Y_+\tilde{F}_2 \mp Y_- x\tilde{F}_3 - y^2\tilde{F}_L\right] , \quad (1)$$

where α is the fine structure constant and the helicity dependences of the electroweak interactions are contained in the functions $Y_\pm \equiv 1 \pm (1-y)^2$. The dominant contribution to the cross-section comes from the structure function $\tilde{F}_2$. The $\tilde{F}_L$ contribution is largest at high y and is expected to diminish with increasing Q^2, whereas the structure function $x\tilde{F}_3$ contributes in the high Q^2 regime of Z^0 exchange. Note that for unpolarized beams, $\tilde{F}_2$ is the same for electron and for positron scattering, while the $x\tilde{F}_3$ contribution changes sign as can be seen in eq. 1. For simplicity it is convenient to present the NC "reduced cross-section" $\tilde{\sigma}_{NC}(x,Q^2) \equiv \frac{1}{Y_+}\,\frac{Q^4}{2\pi\alpha^2}\,x\,\frac{\mathrm{d}^2\sigma_{NC}}{\mathrm{d}x\mathrm{d}Q^2}$

The leading order double differential charged current (CC) cross-section for $e^- p \to \nu X$ may be written as

$$\frac{\mathrm{d}^2\sigma^-_{CC}}{\mathrm{d}x\,\mathrm{d}Q^2} = \frac{G_F^2}{2\pi x}\left(\frac{M_W^2}{M_W^2+Q^2}\right)^2 x\left[(u+c) + (1-y)^2(\bar{d}+\bar{s})\right] , \quad (2)$$

where G_F is the Fermi coupling constant, and u, c, $\bar{d}$, $\bar{s}$ are the quark distributions of the proton. The description of $e^+ p \to \bar{\nu} X$ is obtained by exchanging all quarks with anti-quarks (and vice-versa) in eq. 2. The CC reduced cross-section is defined as $\tilde{\sigma}_{CC}(x,Q^2) \equiv \frac{2\pi x}{G_F^2}\left(\frac{M_W^2+Q^2}{M_W^2}\right)^2 \frac{\mathrm{d}^2\sigma_{CC}}{\mathrm{d}x\mathrm{d}Q^2}$.

The single differential cross-sections $\mathrm{d}\sigma/\mathrm{dQ}^2$ for NC and CC are shown in fig.1 for $y \leq 0.9$. The measurements show the now published e^+p data [2], and new preliminary measurements of the e^-p data [3]. The positron data were taken at $\sqrt{s} \approx 300$ GeV, whilst the electron data were taken at $\sqrt{s} \approx 320$ GeV. The data are compared to the NLO QCD fit performed on low Q^2 fixed target data from NMC and BCDMS and H1 e^+p data, called "H1 e^+p QCD fit" in the following. The new e^-p NC and CC measurements presented here were not included in the QCD fit.

The data are generally found to be in good agreement with the expectation, though an excess of approximately two standard deviations remains at the highest Q^2 in the NC e^+p data. For $Q^2 > 3\,000$ GeV^2 the NC e^-p cross-section is observed to be systematically larger than the e^+p cross-section. The influence of the increased centre-of-mass energy is indicated by the dashed line and predicts an increased cross-section of $\approx 7\%$ for $Q^2 < 1\,000$ GeV^2 rising to 50% at $Q^2 = 30\,000$ GeV^2. However, at high Q^2 this is approximately an order of magnitude smaller than the increase expected from the different lepton charge. The differences between the e^-p and e^+p cross sections are consistent with the SM expectation of the parity violating contribution of Z^0 exchange.

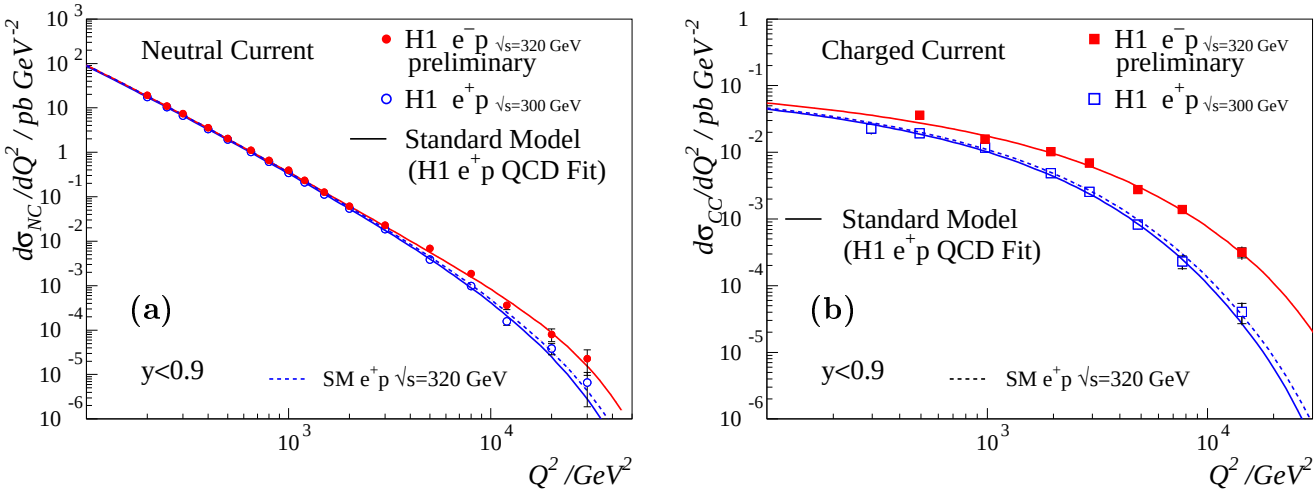

Figure 1: The Q^2 dependences of the NC (a) and CC (b) cross-sections $d\sigma/dQ^2$ are shown for the preliminary e^-p (solid points) and published e^+p (open points) measurements. The data are compared to the SM expectation. The influence of the increased centre-of-mass energy is shown as the dashed curve.

The Q^2 dependence of the CC cross-section for e^+p and e^-p scattering is shown in fig.1b. The electron data are found to have a larger cross section everywhere, by up to a factor of ten at $Q^2 = 15\,000\text{GeV}^2$. The effect of the increased centre-of-mass energy is expected to be relatively small, and is shown as the dashed curve in fig.1b. The CC cross-sections are in good agreement with the SM expectation based on the H1 e^+p QCD fit. The Q^2 dependence of the cross-section at high Q^2 is largely due to the effect of the electroweak propagator and is therefore sensitive to M_W. Fitting the e^+p data for the propagator mass yields the value $M_W = 80.9 \pm 3.3$ (stat.) ± 1.7 (syst.) ± 3.7 (theo.) GeV. The theoretical uncertainty (theo.) is evaluated by varying the input assumptions and the data entering the fit. At the present level of precision, there is no evidence for any anomalous behaviour and the value of M_W extracted is in agreement with time-like determinations [4]. Thus the results are consistent with the expected electroweak structure of the standard model in this newly probed deeply space-like region.

The double differential NC reduced cross-sections for e^+p and e^-p are shown in fig.2(a) which reaches up to $x = 0.65$ and $Q^2 = 30\,000$ GeV^2. The data are compared to the H1 e^+p QCD fit, which is found to give a good prediction of the x, Q^2 behaviour of the data. The two data-sets differ in the manner expected from parity violating contributions. These differences will allow a determination of the $x\tilde{F}_3$ structure function at high Q^2 for the first time.

The double differential CC reduced cross-sections from electron and positron scattering are shown in fig.2(b). The data are well described by the H1 e^+p QCD fit. The cross-sections measured in e^-p scattering are found to be consistently larger than for e^+p scattering. The difference in the cross-sections is found to increase with Q^2. This is expected within the Standard Model and is due to the different quark densities probed in e^+p and e^-p scattering. Thus the CC cross-section is a powerful tool in refining our understanding of the flavour composition of the proton. With increased statistics, these are likely to become the definitive measurements. All of the H1 very high Q^2 data will improve considerably in both statistical precision and coverage of kinematic phase space as higher luminosity becomes available following the HERA upgrade.

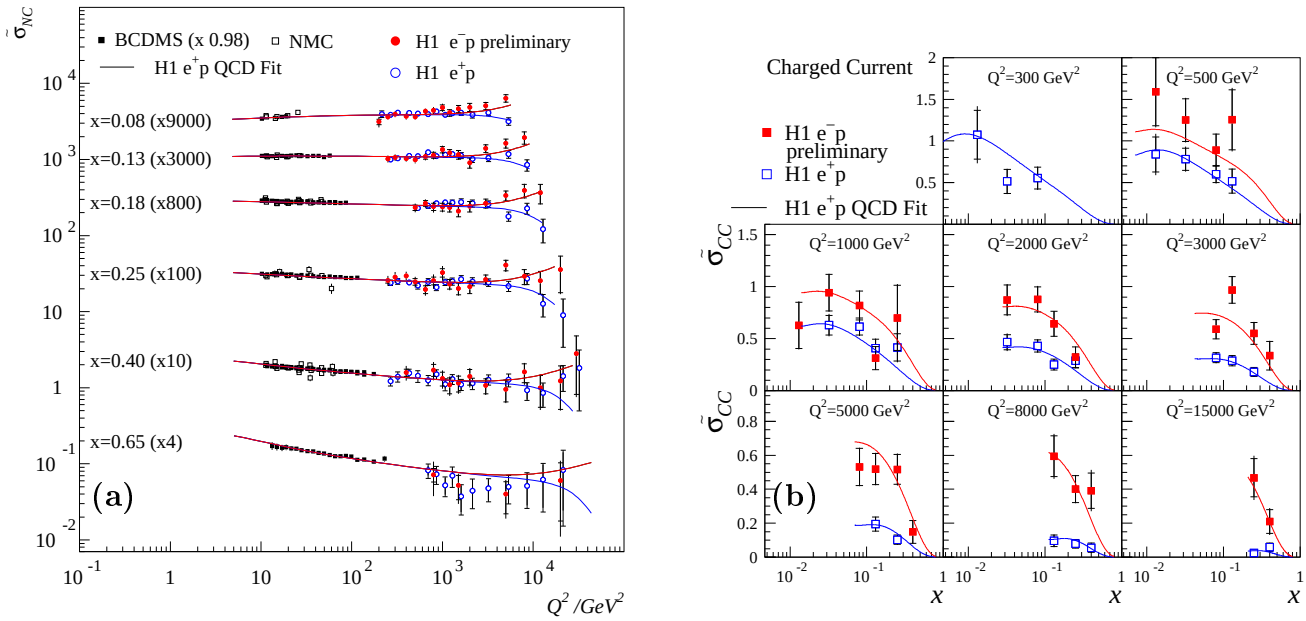

Figure 2: **(a)**The NC reduced cross-section $\tilde{\sigma}_{NC}$ is shown at high x for the preliminary e^-p data ($\sqrt{s} \approx 300$ GeV, solid points) and the e^+p data ($\sqrt{s} \approx 320$ GeV, open points) compared to the SM expectation. **(b)**The CC reduced cross-section $\tilde{\sigma}_{CC}$ is shown for the preliminary e^-p data ($\sqrt{s} \approx 300$ GeV, solid points) and the e^+p data ($\sqrt{s} \approx 320$ GeV, open points) compared to the SM expectation.

2.2 W Production

In the Standard Model W bosons are produced at HERA predominantly in photoproduction via bremsstrahlung off a quark ($ep \to eWX$). In certain scenarios beyond the Standard Model Ws may be produced via decays of heavier particles. For instance if single top quarks were produced (e.g. via the reaction $\gamma c \to t$, as proposed in [5]) Ws would be observed in the decay $t \to bW$. A similar decay chain occurs in supersymmetric models where the stop decays to W sbottom ($\tilde{t} \to \tilde{b}W$) [6]. In such models the W would be produced alongside a hadronic jet with high transverse momentum.

At H1 W events are identified in the $W \to e\nu$ and $W \to \mu\nu$ decay channels, by selecting events with large missing transverse energy and an isolated electron or muon [7, 8]. A search was carried out using 12.8 pb^{-1} of e^-p scattering data and 36.5 pb^{-1} of e^+p scattering data.

A total of eight W candidate events were found, all of which appeared in the e^+p data sample. Three of these events were observed in the $W \to e\nu$ channel compared to 2.24 ± 0.67 expected from W production and 0.88 ± 0.19 from background sources. The other five candidate events were observed in the $W \to \mu\nu$ channel compared to 0.87 ± 0.26 expected from W production and 0.14 ± 0.09 from other Standard Model sources. In the e^-p data sample, no events were observed, which should be compared with 2.0 events expected from Standard Model processes.

The excess of events in the muon channel is even more striking when the events are studied as a function of P_T^X, the transverse momentum of the hadronic jet, as listed in table 1. At low P_T^X there is no significant deviation from the Standard Model. At $P_T^X > 40$ GeV 3 muon events are observed compared to a Standard Model expectation of 0.60 (e^+ and e^-, e and μ decay channels combined). The large increase in luminosity after the HERA upgrade will quickly allow us to investigate this signal with higher statistics.

Electron	Data	SM expectation	W
$P_T^X > 0$ GeV	3	3.12 $\pm$0.70	2.24 $\pm$0.67
$P_T^X > 12$ GeV	1	1.15 $\pm$0.25	0.78 $\pm$0.23
$P_T^X > 40$ GeV	0	0.16 $\pm$0.04	0.14 $\pm$0.04
Muon	Data	SM expectation	W
$P_T^X > 12$ GeV	5	1.01 $\pm$ 0.28	0.87 $\pm$ 0.26
$P_T^X > 40$ GeV	3	0.21 $\pm$ 0.06	0.19 $\pm$ 0.06

Table 1: Observed and predicted event rates in the electron and muon decay channels of the W for e^+p data.

2.3 Diffractive Hard Scattering

The UK has traditionally been at the forefront of the H1 investigation into diffractive phenomena. This remains a fast developing field, with significant developments in the perturbative QCD (pQCD) description of hard diffraction in recent years. Experimentally, diffractive events are characterised by large regions of the detector in which there is no activity, a 'rapidity gap'.

The cross section for the process $\gamma^* p \to Xp$, where the photon dissociative system X is separated from the proton by a large rapidity gap, has been measured by H1 in the form of a diffractive structure function $F_2^{D(3)}$ [9]. The diffractive structure function has been used to test diffractive factorisation hypotheses. The hard component of the diffractive DIS scattering amplitude has recently been shown to be factorisable [10], just as in standard DIS. Factorisation can be taken further under the assumption, inspired by Regge phenomenology, that there is a universal flux of an object with vacuum quantum numbers (the pomeron) associated with the proton [11]. Under this assumption, the parton distributions of the pomeron have been extracted from F_2^D data [9].

A major activity at HERA over the past years has been the testing of the validity of these parton distributions for the description of as many diffractive observables at HERA as possible. The two measurements described below provide perhaps the most stringent tests yet. They are both directly sensitive to the diffractive gluon distribution, which can only be inferred from scaling violations in more inclusive analyses. A still more exacting test of the factorisable pomeron picture comes when the pomeron parton distributions from HERA are used to predict cross sections at other colliders, in particular the Tevatron. Here the picture runs into serious trouble, where HERA based predictions can fail by factors of order 100 for certain processes [12]. The development of a phenomenological understanding of this failure of factorisation has become a major challenge for QCD.

2.3.1 Diffractive Dijet Electroproduction

The generic diffractive process at HERA is shown in figure 3. Under the Regge factorisation ansatz, with the proton remaining intact, figure 4 represents the dominant dijet producing process at leading order of QCD. A gluon from the pomeron undergoes boson-gluon fusion with the virtual photon, such that the outgoing q and $\bar{q}$ may have high transverse momentum. The variable $z_{I\!P}$ then represents the fraction of the pomeron momentum that enters the hard scatter. A hadron level estimator of this quantity, $z_{I\!P}^{jets}$, is defined as

$$z_{I\!P}^{jets} = \frac{M_{12}^2 + Q^2}{M_X^2 + Q^2} \tag{3}$$

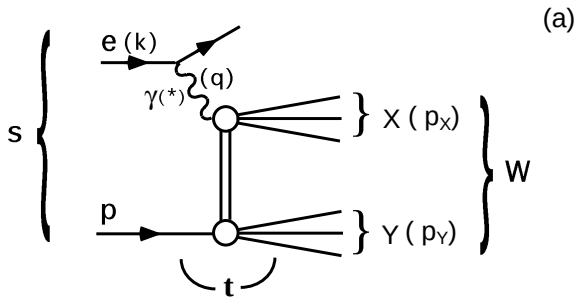

Figure 3: The generic diffractive process at HERA

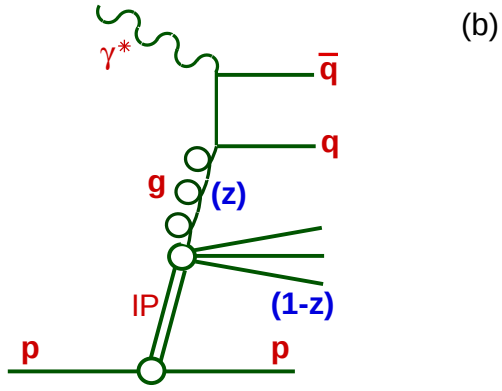

Figure 4: The dominant leading order QCD process for diffractive dijet and charm production in the partonic pomeron model.

where M_{12} and M_X are the invariant masses of the dijet system and the full system X respectively.

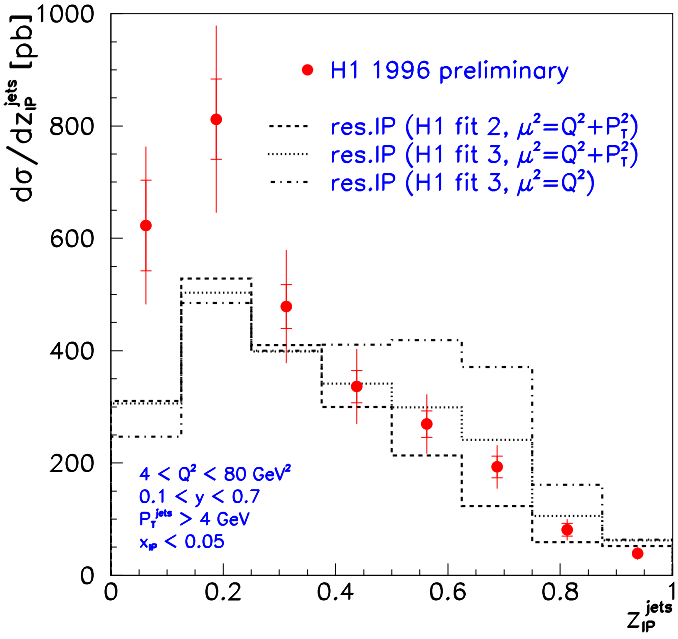

Figure 5: Differential hadron level cross section for diffractive dijet production as a function of $z_{I\!P}^{jets}$. The data points are shown with the predictions from a partonic pomeron model with different choices of the pomeron parton distribution functions and factorisation scales.

The kinematic region probed in this analysis is determined to a large extent by the requirement that there be at least 2 jets in the X system. This forces the invariant mass of the X system to be large, and $z_{I\!P}$ typically to be small. Indeed, the fractional momenta accessed extend to values lower than those reached in inclusive analyses. Figure 5 [13] shows the corrected $z_{I\!P}^{jets}$ distribution compared, via a Monte Carlo model, with two different sets of pomeron parton distributions (labelled *fit 2* and *fit 3*) extracted by H1 from analysis of $F_2^{D(3)}$ [9], for two choices of factorisation scale μ. In terms of overall normalisation and general shape, the agreement between the factorisable pomeron model and the data is rather good, particularly since the kinematic ranges, experimental method and systematics are very different between the two cases. There is evidence from the jet data of a need to modify the parton densities in

the low $z_{I\!P}$ region, and some sensitivity to the appropriate choice of parton distributions and factorisation scale. According to the models, approximately 75% of the dijet cross section can be attributed to hard scattering processes involving gluons from the pomeron.

2.3.2 Diffractive Electroproduction of $D^{*\pm}$ Mesons

Within the resolved pomeron model, the production of open charm occurs via the same mechanism as the dijets (figure 4), where the quarks emerging from the boson-gluon fusion process are a $c\bar{c}$ pair. The process has also been modelled using a pQCD approach to the pomeron structure based on 2-gluon exchange [14].

An analysis [15] has been performed using data collected during 1995, 1996 and 1997, corresponding to an integrated luminosity of $20.8\text{pb} - 1$. The D^{*+} mesons are reconstructed using the decay channel

$$D^{*+} \rightarrow D^0 \pi^+_{slow} \rightarrow (K^- \pi^+)\pi^+_{slow} \tag{4}$$

which has a branching ratio of 2.63%. The cross section in the kinematic range[1] $2 < Q^2 < 100GeV^2$, $0.05 < y < 0.7$, $x_{I\!P} < 0.04$, $M_Y < 1.6\text{GeV}$, $|t| < 1\text{GeV}^2$, $p_T(D^{*\pm}) > 2\text{GeV}$ and $|\eta(D^{*\pm})| < 1.5$ is

$$\sigma(ep \rightarrow (D^{*\pm}XY) = 154 \pm 40(stat.) \pm 35(syst.)\text{pb}. \tag{5}$$

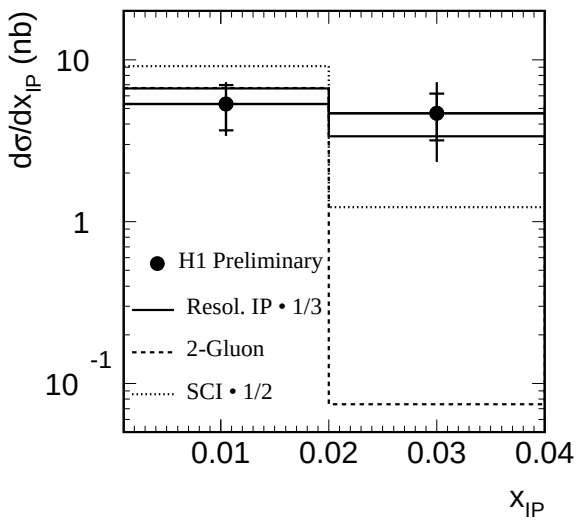

Figure 6: The cross section $\sigma(ep \rightarrow D^{*\pm}XY)$ measured differentially in $x_{I\!P}$.

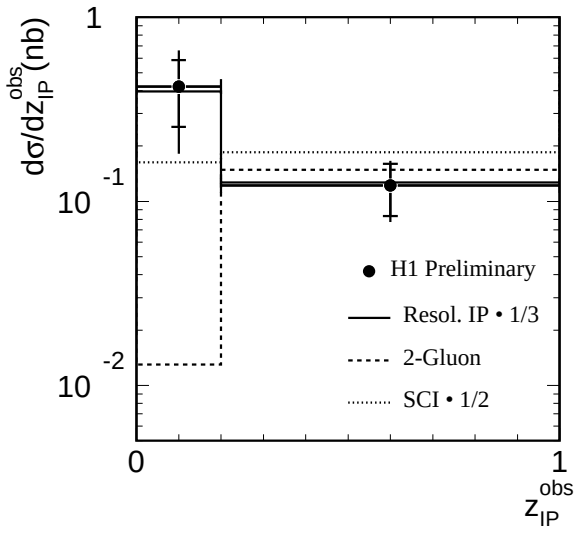

Figure 7: The cross section $\sigma(ep \rightarrow D^{*\pm}XY)$ measured differentially in $z^{obs}_{I\!P}$.

The cross section is shown differentially as a function of $z^{obs}_{I\!P}$ and $x_{I\!P}$ in figures 6 and 7. The 2-gluon model fails in the regions of higher mass for system X, i.e. low $z^{obs}_{I\!P}$. This behaviour is reflected in the failure at high $x_{I\!P}$. This indicates that refinements of the model are necessary. At present, only the case in which the parton level final state system X consists exclusively of a $c\bar{c}$ pair is implemented. In the regions where the X system must have this basic parton level configuration (high $z^{obs}_{I\!P}$), the model successfully predicts the magnitude of the cross section. Calculations where $c\bar{c}g$ final states are also considered must be included in order to describe the low $z^{obs}_{I\!P}$ region.

[1]Here, $x_{I\!P}$ is the fraction of the proton beam energy that is exchanged to the system X, t is the square of the four-momentum transferred, M_Y is the mass of the dissociating proton system where the proton does not remain intact and y is the standard Bjorken scaling variable.

The partonic pomeron model predicts the shape of all the differential distributions well (further differential distributions can be found in [15]). The overall normalisation fails by a factor of 3, however. This effect may be the first indication of a failure of the partonic pomeron model. The large increases in statistics that are likely to be available after the upgrade will resolve this question.

2.4 Diffractive Vector Meson Production

The elastic and quasi-elastic production of vector mesons provide a useful testing ground for models of diffraction. While Regge theory with a soft pomeron describes photoproduction of light vector mesons well, processes where either Q^2 or the meson mass is larger show a steeper energy dependence [16–18]. In perturbative QCD (pQCD), which is expected to be valid for sufficiently large Q^2 or mass, this behaviour is driven by the increase in the gluon density of the proton as x decreases.

2.4.1 Elastic J/ψ Electroproduction

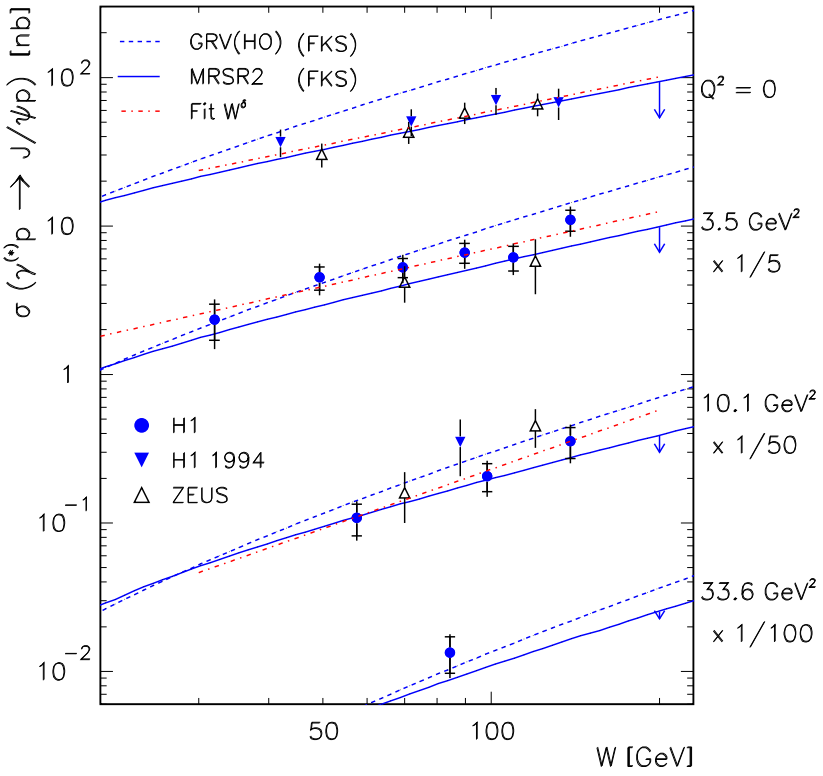

Figure 8: Cross sections for elastic J/ψ production as a function of W at different values of Q^2, measured at HERA. The cross section at $\langle W \rangle = 32\,\mathrm{GeV}$ and $Q^2 = 3.5\,\mathrm{GeV}^2$ was measured using events in which one of the muons from the decay $J/\psi \to \mu^+\mu^-$ was detected in the FMD.

Figure 8 shows photon-proton cross sections for elastic J/ψ production, $\gamma^* p \to J/\psi\, p$, as a function of the centre-of-mass energy W for several values of the photon virtuality Q^2. The data can be described by QCD models (e.g. [19], labelled 'FKS' in the figure) based on the exchange of gluon pairs from the proton. The results [16] use data from 1995 to 1997 to provide more

precise measurements in a larger kinematic range then earlier analyses. The Forward Muon Detector (FMD) has been used to extend the coverage to lower energy, $\langle W \rangle = 32.0\,\mathrm{GeV}$, at $Q^2 = 3.5\,\mathrm{GeV}^2$. This has the advantage of narrowing the gap in energy between the other results from HERA and those from fixed-target experiments, and enables an investigation of the energy dependence which is independent of other experiments. To measure this data point, events were used in which one muon from the decay $J/\psi \to \mu^+\mu^-$ was reconstructed in the FMD while the other was identified using the Liquid Argon Calorimeter or the Central Muon Detector. A sample of events with both muons in the FMD was used as a check on the detector efficiency. Mass spectra for both samples are shown in figure 9.

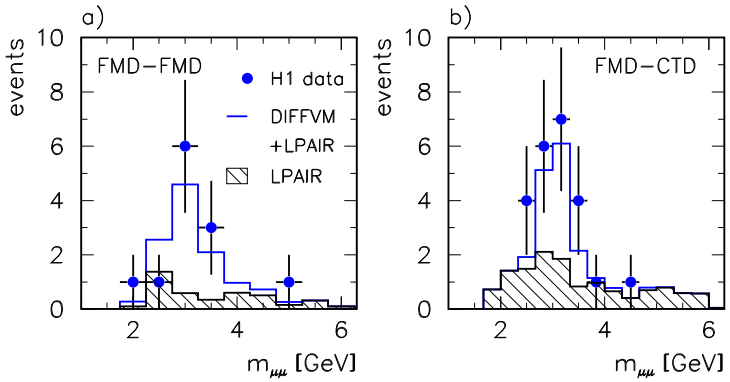

Figure 9: Mass spectra from events in the low-W J/ψ sample. (a) Events with both muons in the FMD. (b) Events with one muon in the FMD and the other in the central region, used in the published measurement. The uncorrected data are compared with the sum of a diffractive J/ψ production model (DIFFVM) and a contribution (LPAIR) from the background process $\gamma\gamma \to \mu^+\mu^-$.

2.4.2 Elastic J/ψ Photoproduction

The strong W dependence of the elastic J/ψ photoproduction cross section is now clearly established, with ever more precise data becoming available [18]. This strong rise is incompatible with the pomeron of soft hadronic physics and encourages a perturbative QCD treatment.

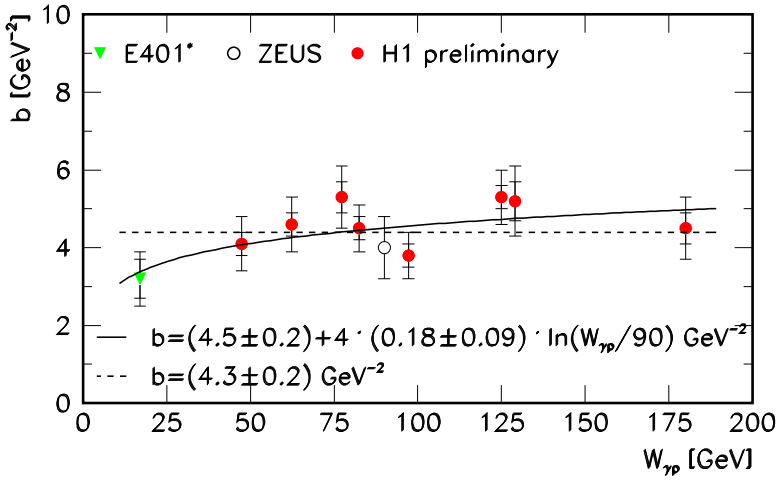

Figure 10: H1 result for the exponential slope parameter b in fits to the t distribution in J/ψ photoproduction, shown as a function of W, together with a modified fixed target result. The dashed line shows the best fit to the H1 data assuming the absence of shrinkage. The solid line shows the best fit in which shrinkage is allowed.

A further signature for perturbatively tractable behaviour would be the absence of significant shrinkage of the forward elastic peak with increasing centre of mass energy. The t dependence of the elastic J/ψ production cross section has been studied as a function of W to see if shrinkage could be established [18]. Combining the H1 data with the appropriate data from fixed target experiments allowed the W dependence of the slope of the diffraction peak to be investigated. Figure 10 shows the value of the slope parameter b plotted as a function of W, when the data in each W bin are fitted to the form e^{bt}. The precision of the data is not yet sufficient to allow a strong statement on the presence or absence of a W dependence of b. A paper is presently in preparation, which extends this analysis to the direct extraction of the effective Regge trajectory describing the elastic J/ψ photoproduction process.

2.5 Open Beauty Production

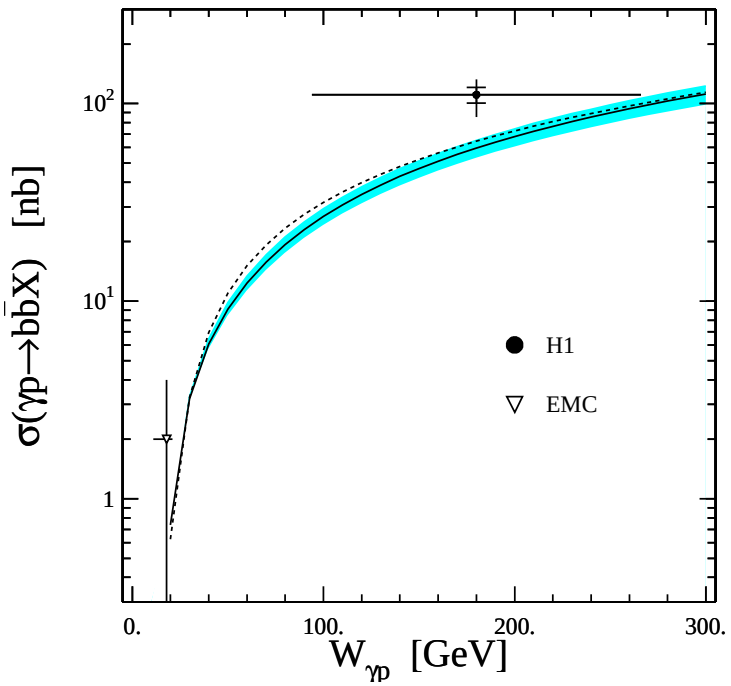

Figure 11: H1 and EMC results on the total photoproduction cross section for the process $\gamma p \to b\bar{b}X$. The curves represent NLO QCD calculations with varying choices for the parton distributions of the proton, the factorisation and renormalisation scales.

Due to the very small production cross sections, the study of beauty production at HERA has barely begun. The first H1 measurement of open beauty photoproduction has recently been published [20]. The technique used was to select an enriched sample of semi-leptonic b decays on the basis of muons with a $p_T > 2$ GeV embedded within jets. The sample contained about 50% b events with 50% background with equal contributions from the semi-leptonic decay of charm and from light hadrons. These backgrounds were measured from the data and subtracted to obtain the beauty signal. The total leptoproduction and photoproduction cross sections were measured from the 1996 data. Figure 11 shows the result, which is somewhat above the value expected from the photon-gluon fusion process computed at Next-to-Leading Order of QCD. The higher luminosity data from 1997 and beyond are being used to check this result and measure the beauty production cross sections as a function of kinematic variables such as W and Q^2.

2.6 Strange Particle Production

The flavour structure of the hadronic final state contains information about the partonic composition of the proton and sheds light on the hadronisation process. The H1 collaboration has recently made the first measurements of charged kaon and pion production in the low x domain [21]. Figure 12 shows the differential transverse momentum spectra $\frac{1}{N}\frac{dn}{dp_T^{*2}}$ of charged kaons inclusively produced in DIS interactions. The rate reduces as the transverse momentum increases.

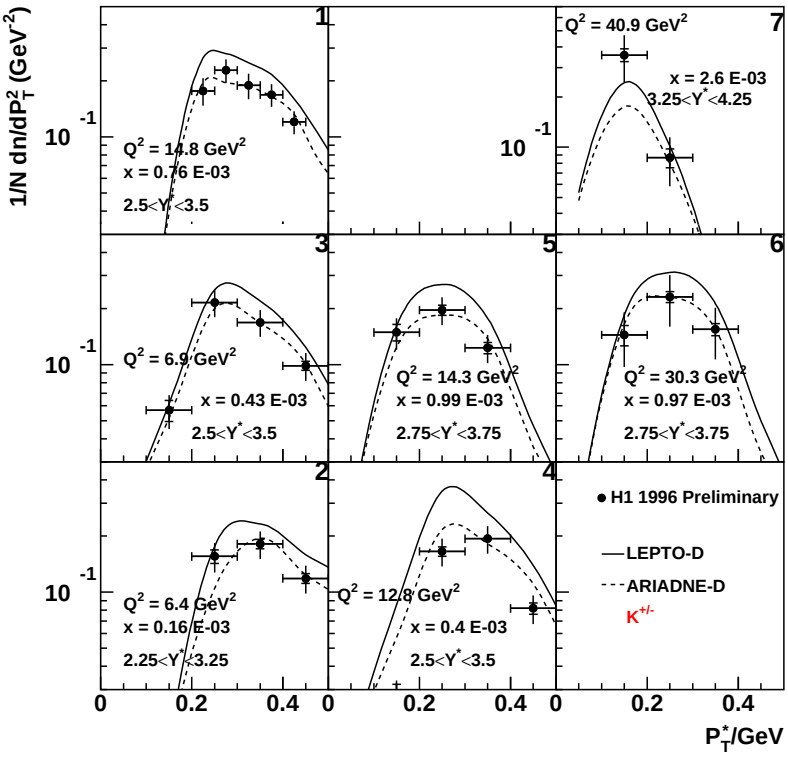

Figure 12: The inclusive charged kaon distributions $\frac{1}{N}\frac{dn}{dp_T^{*2}}$ in different intervals of x and Q^2. The predictions of QCD-based models are also shown.

There is no large dependence on the kinematics of the DIS interaction. QCD-based models which use a string fragmentation approach determined from e^+e^- data are compared with the data. These models describe the data well, thereby supporting the hypothesis of the environmental independence of hadronisation. The value of the 'suppression factor' in low x DIS, corresponding to the ratio of probabilities of vacuum production of $s\bar{s}$ pairs to the lighter $u\bar{u}$ and $d\bar{d}$ pairs, $\mathcal{P}(s\bar{s})/[\mathcal{P}(u\bar{u}) + \mathcal{P}(d\bar{d})]$ was found to be approximately 0.23.

2.7 Fragmentation Functions and Rapidity Spectra in the Breit Frame

Studies of DIS ep processes in the Breit frame of reference by H1-UK groups have recently been published [22–24]. These have included the energy dependence of the moments of the fragmentation function, invariant energy spectra and the correlation between the charge of the hadronic final state and the charge of the scattered parton [25]. Two highlights of this year's work are described below.

2.7.1 Scaling Violations

In figure 13, the fragmentation function is plotted in intervals of the scaled momentum variable, x_p, as a function of the invariant four-momentum transfer, Q. The function shows a strong rise at small x_p with increasing energy which becomes flatter in the larger x_p region. Predictions based on NLO QCD calculations [26] (dotted line) have a tendency to overestimate the inclusive particle production cross section in the small x_p, low Q region where the available phase space for fragmentation is strongly suppressed.

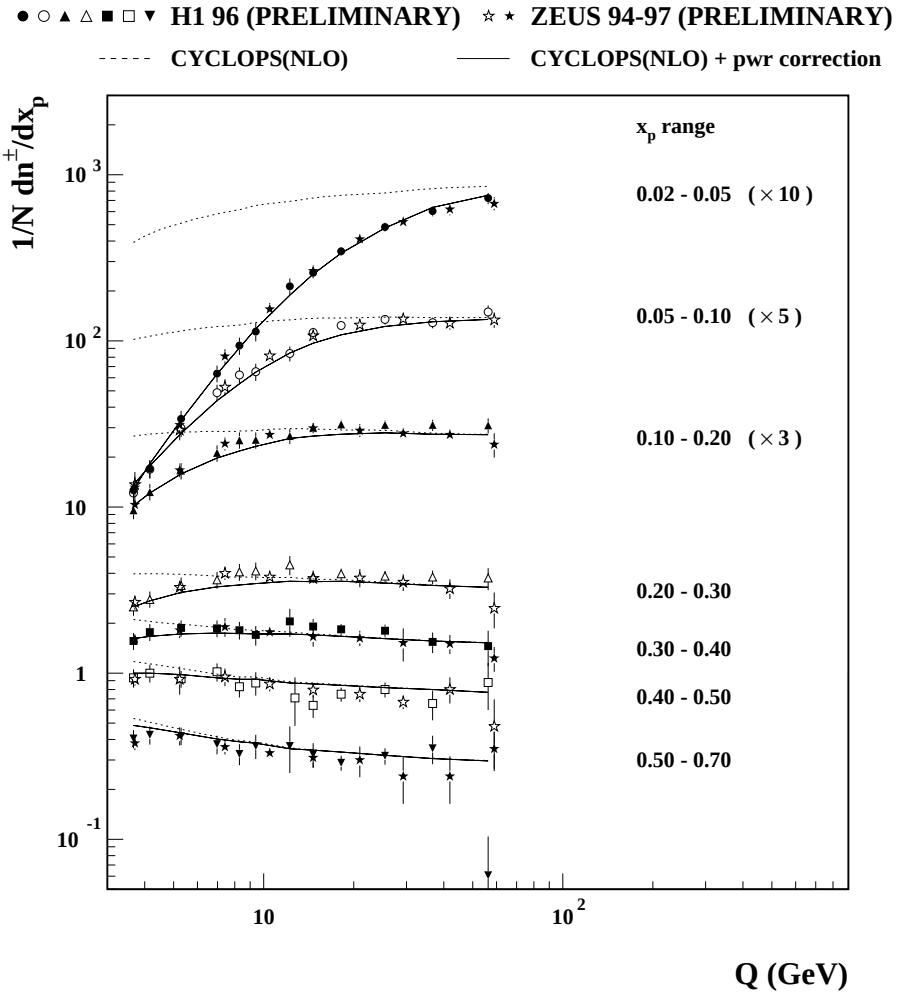

Figure 13: H1 and ZEUS fragmentation function measurements, plotted for different intervals of x_p as a function of Q^2. Note that the data for the three smallest intervals of x_p are scaled by factors of 10, 5 and 3 for clarity. The dotted and solid lines show the predictions of the 'CYCLOPS' NLO QCD calculation with and without the power correction respectively.

These "mass effects" are neglected in the pQCD approach but may be taken into account by means of a "power-correction" factor of the form

$$F = \left(1 + \left(\frac{\mu}{p_h}\right)^2\right)^{-1}$$

Here, p_h is the momentum of the final state hadron and μ is a free parameter that sets the hadronic mass scale. The solid line in figure 13 shows the result of applying this correction ($\mu = 300$ MeV) to the NLO calculation. The agreement with the H1 ep data over the available phase space is remarkable.

2.7.2 Rapidity Spectra

Figure 14 presents the rapidity spectra [27] for high Q^2 data integrated over all transverse momenta, and binned in various p_t intervals. The proton remnant extends toward large positive rapidity. At low p_t a clear plateau in the target hemisphere can be seen. As the average p_t of the particles increase, QCD effects gradually evolve the flat plateau into an almost Gaussian structure peaking near the origin of the Breit frame axis ($Y = 0$).

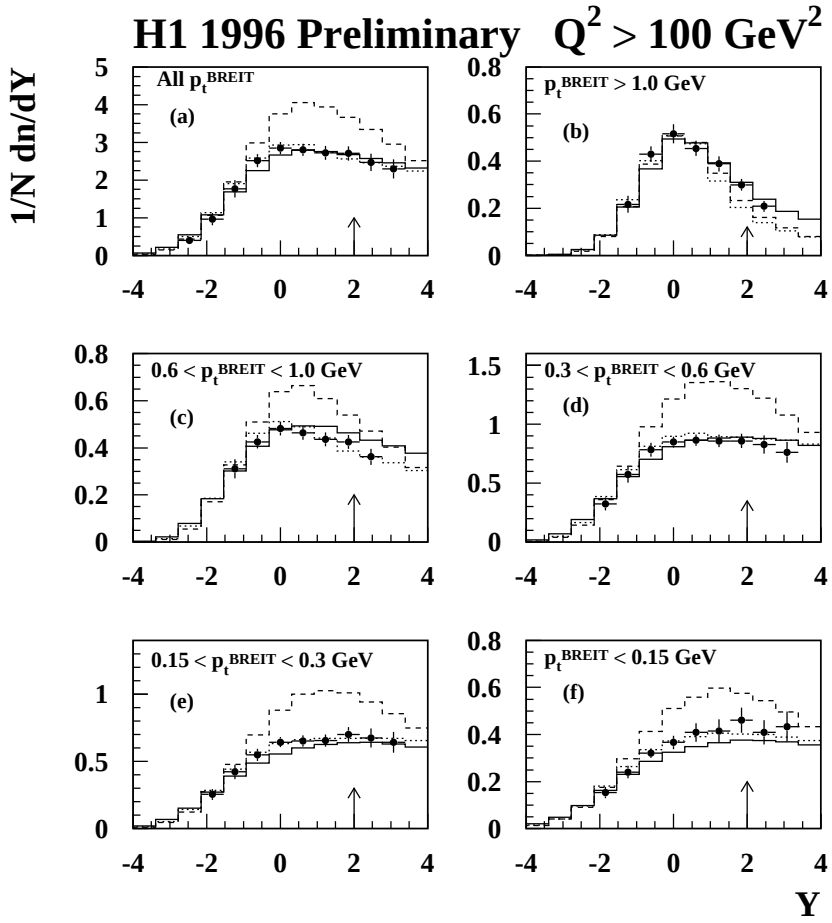

Figure 14: The rapidity distribution in the Breit frame for (a) all charged tracks and (b-f) the five indicated intervals of track transverse momentum, p_t^{BREIT}, all at high Q^2. The error bars show the sum of statistical and systematic errors added in quadrature. The arrow indicates the position of the origin of the hadronic centre of mass system for the $< Q >$ (23 GeV) of the data. The histograms show the predictions of Monte Carlo models based on leading order QCD, the solid line utilising a colour dipole fragmentation, the dashed (dotted) lines utilising a parton shower with (without) soft colour interaction effects.

Predictions based on Local Parton Hadron Duality suggest the presence of two distinct plateaux with a 9/4 ratio in their respective heights reflecting the colour charge of the dominant gluonic radiation in the target hemisphere [28] as opposed to the exchange quark in the current

region. Despite many tests to isolate events in which such behaviour might be expected to be amplified, we have been unable to observe a double plateau structure.

3 Detector Status and Developments

All the detector components described below remain the principal responsibility of UK groups. During HERA running periods each device requires more or less continuous attention from dedicated physicists, either directly at DESY or remotely from the UK via computer link.

3.1 Data Acquisition and Silicon Tracker Readout

During 1999 the data acquisition and readout systems continued to operate and perform reliably. These systems, which are based on the VMEbus standard, have been described extensively in previous annual reports. Optical fibres are used to interconnect over 100 electronics crates containing the necessary ADCs and several hundred microprocessors. The introduction of the PCI standard has considerably enhanced the system potential which, together with Power PC technology, has resulted in more compact solutions performing at increased data throughput rates.

Preparations are now being made for the expansion of the RAL-designed Silicon Readout System to cater for more detector components, namely the Forward Silicon Tracker. This will result in nearly 3/4 million total silicon channels being read out by the system.

3.2 Backward Calorimeter Timing

The timing electronics and monitoring procedures for the SpaCal lead/scintillating fibre calorimeter have also continued to function reliably during 1999. No particular problems arose from the different operating conditions implied by the changes in lepton beam charge and proton beam energy. During the year QMW physicists provided on-call expert help and contributed to on-going analysis work to improve trigger selectivity and calibration as well as to the publication of a summary paper [29] on this detector.

3.3 Forward Muon Detector and Trigger

The Forward Muon Detector (FMD) and Forward Muon Trigger have performed smoothly during 1999, despite a couple of hardware problems. The system has been maintained by the Birmingham and Manchester groups. The currents drawn by the sense wires in the FMD drift chambers have increased in line with the increased beam currents injected by HERA. Hardware problems occurred with a mass flow meter responsible for determining the gas mixture and with a CAEN HV module; it emerged that the chambers had been damaged but, after a detailed study, it was concluded that the damage was not permanent. No effect on track reconstruction was observed, and since the effect was in a post-toroid layer, it did not interfere with the use of the pre-toroid layers as a veto for diffraction analyses.

In 1999 the H1 publication on charmonium production [16] in DIS included a cross section for low W elastic production of J/Psi measured using the FMD. A similar measurement for photoproduction is to be included in a forthcoming H1 paper.

3.4 Forward Track Detector

The Forward Track Detector (FTD) has performed well during most of 1999 under the direct control of UK physicists resident at DESY, with monitoring and calibration in the hands of UK based scientists via remote computer link.

In October a serious leak occurred in the cooling system between the Central and Forward Track Detectors. In order to keep the temperature of the detector-mounted pre-amplifiers of both the FTD and the central tracker within safe limits, it proved necessary to run without power to the FTD Radial chambers. The resulting 7% loss in FTD track finding efficiency and 15% degradation in precision are unfortunate but unavoidable consequences of that safety requirement, which ensures that the electronic and structural components of the FTD chambers survive undamaged for the upgrade. Repair of the leak will take place during the next HERA shut-down.

4 Upgrade Projects

The UK groups are responsible for two major projects for the forthcoming upgrade, which will ensure that we exploit fully the increased luminosity after 2001.

4.1 Forward Track Detector Upgrade

There were significant developments in the programme to upgrade the H1 Forward Track Detector (FTD) [30] during 1999. Firstly, the design of the structure that will support the GO magnet that is to extend through the foremost two thirds of the FTD was completed; the support required will be mounted between the Central and Forward Track Detectors and can only be accommodated if the FTD is shortened somewhat. Secondly, as the operation of the Planars proved to be more stable than that of the Radials during high background positron-proton running, the decision was taken to remove not only the MWPCs and the Transition Radiators from the FTD, but also the Radials and use the space so created to insert not three new Planars, as originally planned, but five. The resulting upgraded FTD design is shown in figure 15. Note that the new Planars contain 8 sense wires as opposed to the 4 wires in the original chambers. This aids resolution of the left-right ambiguity and further improves the pattern recognition capabilities of the FTD. The design of the new Planars was completed early in the year and construction started at Daresbury once the necessary clean room space had been built. Two chambers have now been constructed and are under test. The Daresbury team can produce two chambers a month, allowing the comfortable completion of the chambers required for installation in H1 within the HERA upgrade schedule.

The software needed for the simulation, readout and calibration of the upgraded FTD is being developed in parallel with the construction of the new Planars, as is the necessary reconstruction code.

4.2 Track Trigger Upgrade

A high resolution Fast Track Trigger (FTT) [31] is being built for implementation in H1 after the luminosity upgrade in 2000 in order to extend the triggering capabilities for exclusive final states involving tracks. This is aimed at enhancing the trigger efficiency for exclusive physics in the absence of any high p_t particles, thus allowing precision measurements of rare processes such as D^* production using the high post-upgrade luminosity. The project represents one of the most ambitious attempts to reconstruct tracks with high precision down to low p_t in the real

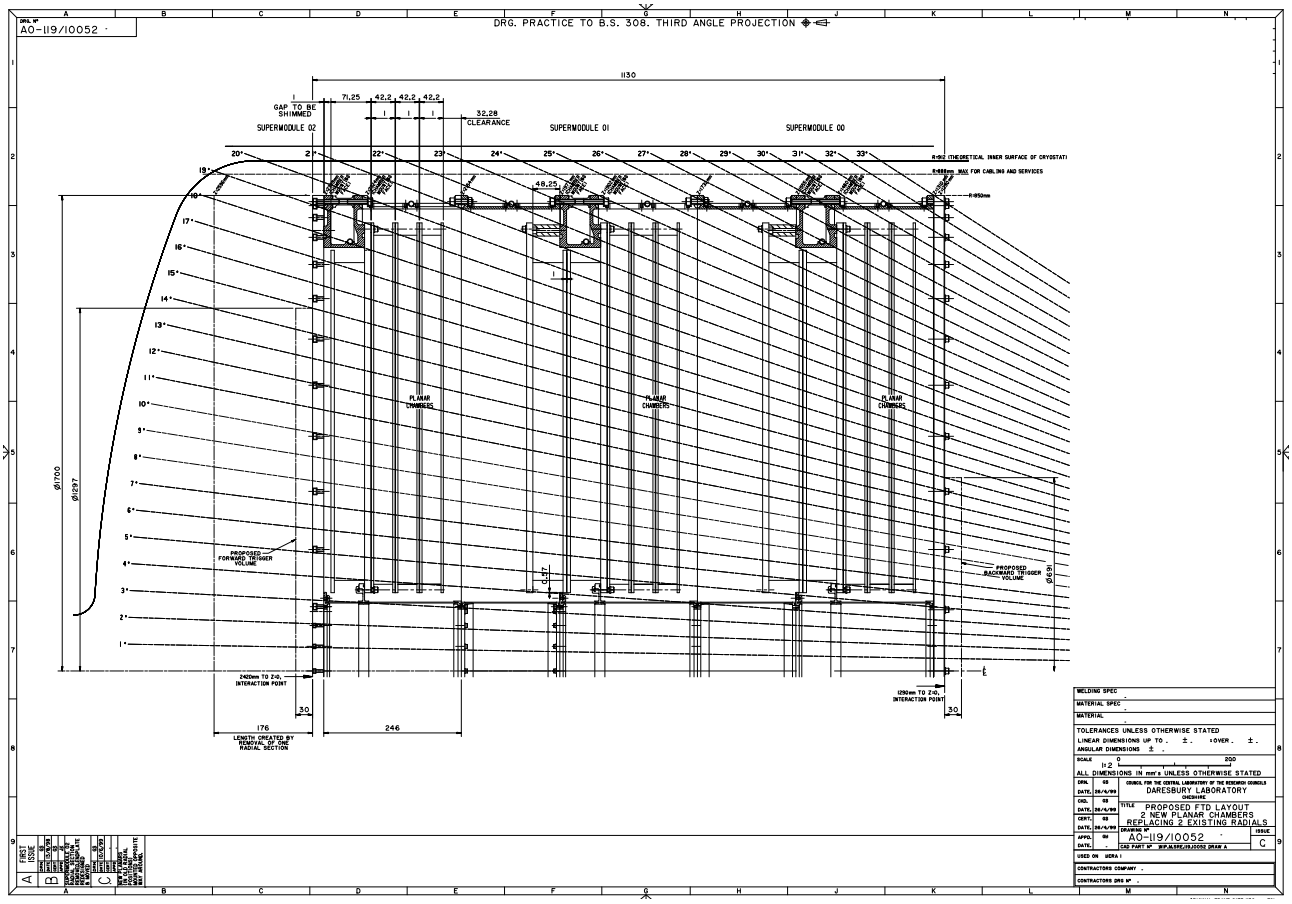

Figure 15: The plans for the Upgraded Forward Track Detector.

time environment necessary for triggering in high multiplicity events at a collider. Extremely good selectivity is achievable by combining the tracks to form invariant mass calculations.

The aim is to have track information from the Central Jet Chamber with which to make basic selections at the first level trigger (L1), full track based selections at level 2 and kinematic selection using combinations of tracks at level 3 (the latter in around 100 μs). The UK groups have undertaken the design and construction of the L1 part of this system. As illustrated in figure 16, this requires the digitisation of the analogue signals from the drift chamber, highly parallel "Q/t" analysis, local track segment finding in fast FPGA arrays and application of the L1 trigger logic, all within 2.3 μs of the interaction. The segment information is then distributed appropriately for the later track linking and fitting in the L2 system.

A proposal was submitted to the PPESP for its September meeting with an open presentation given at the December meeting.

5 Summary

The UK groups have continued to be prominent in all areas of H1 activity, taking leading roles in physics analysis, detector maintenence and upgrade projects. 1999 saw easily the largest volume of data collected in a single year to date. The analysis of this data is likely to yield many exciting results in the coming years. With the HERA upgrade due to commence in September 2000, still larger luminosities are soon to be expected. The future of the H1

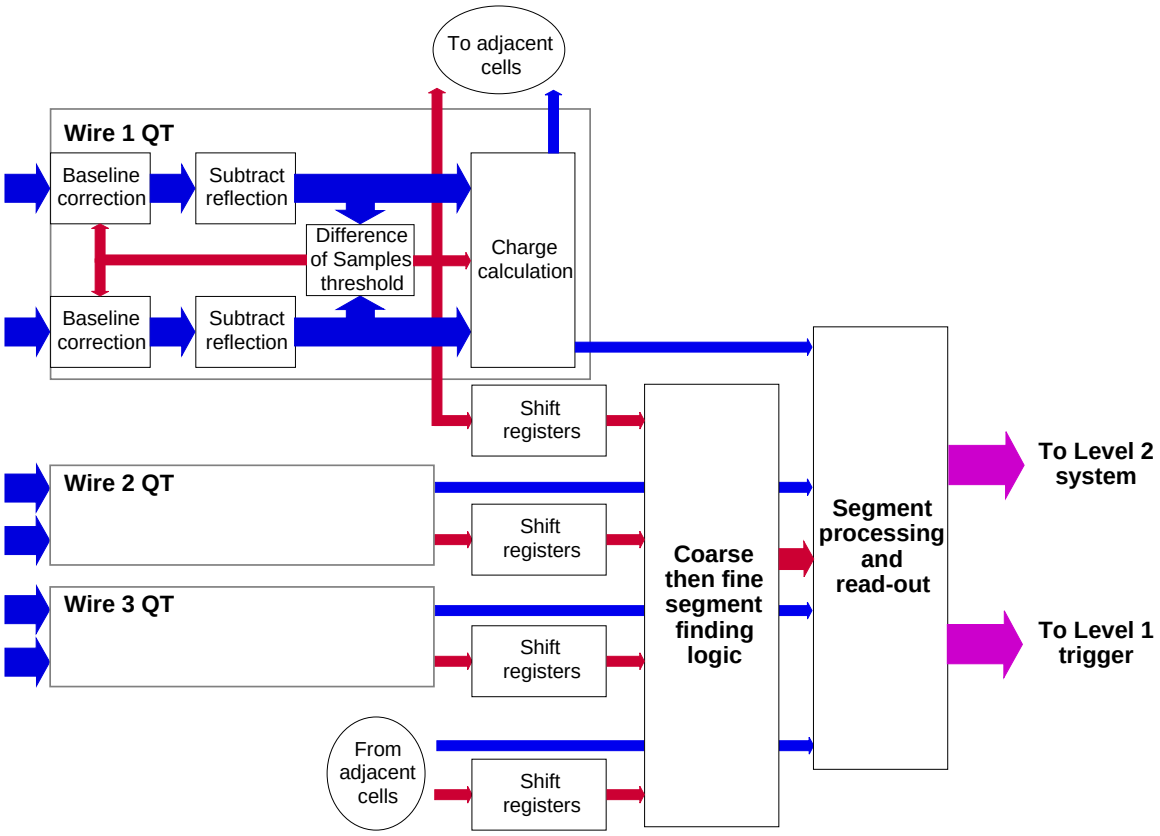

Figure 16: Block diagram of the Fast track Trigger algorithm for finding track segments from groups of three drift chamber wires.

experiment therefore looks bright for several years to come. The UK groups intend to continue to be at the forefront of this cutting edge experiment.

6 H1 Publications 1999

The following papers were submitted to academic journals by the H1 Collaboration between December 1998 and December 1999.

1. "Measurement of D^* Meson Cross Sections at HERA and Determination of the Gluon Density in the Proton", *Nucl.Phys.* **B545** (1999) 21.

2. "Measurement of Dijet Cross-Sections at Low Q^2 and the Extraction of an Effective Parton Density for the Virtual Photon", *DESY* **98-205**, to appear in *Eur. Phys. J.*

3. "Measurement of Internal Jet Structure in Di-jet Production in Deep Inelastic Scattering at HERA" *Nucl.Phys.* **B545** (1999) 3.

4. "Elastic Electroproduction of ρ^0 Mesons at HERA", *DESY* **99-010**, to appear in *Eur.Phys.J.*

5. "Charmonium Production in Deep Inelastic Scattering at HERA", *Eur. Phys. J.* **C10** (1999) 373.

6. "A Search for Leptoquark Bosons and Lepton Flavor Violation in Positron-Proton Collisions at HERA", *Eur. Phys. J.* **C11** (1999) 447.

7. "Measurements of Transverse Energy Flow in Deep-Inelastic Scattering at HERA" *DESY* **99-091**, accepted by *Eur. Phys. J.*

8. "Forward π^0-Meson Production at HERA", *Phys. Lett.* **B462** (1999) 440.

9. "Measurement of Neutral and Charged Current Cross-Sections in Positron-Proton Collisions at Large Momentum Transfer", *DESY* **99-107**, submitted to Eur Phys J.

10. "Measurement of Open Beauty Production at HERA", *Phys. Lett.* **B467** (1999) 156.

11. "Investigation of Power Corrections to Event Shape Variables measured in Deep-Inelastic Scattering" *DESY* **99-193**, submitted to *Eur. Phys. J.*

7 Theses

The following theses concerned with H1 were submitted by students from UK institutes between December 1998 and December 1999.

1. "A Measurement of Jet Cross Sections at Low Q^2 and an Interpretation of the results in terms of a Partonic Structure of the Virtual Photon", Mark Smith (Liverpool).

2. "Open Charm Production in Inclusive and Diffractive Deep-Inelastic Scattering at HERA", Paul Thompson (Birmingham).

3. "The Diffractive Production of J/ψ Vector Mesons with High Transverse Momenta at HERA", Duncan Brown (Manchester).

4. "High Transverse Momentum 2-Jet and 3-Jet Cross Section Measurements in Photoproduction", Paul Bate (Manchester).

8 H1 Conference Presentations 1999

Conference presentations concerned with H1 activities made between December 1998 and December 1999 by members of the UK groups are listed below.

1. E. Rizvi, "Neutral and Charged Current DIS at high Q^2", 13th Topical Conference on Hadron Collider Physics (Hadron13), Mumbai, India, January 1999.

2. A. Mehta, "The Outlook for HERA", 13th Topical Conference on Hadron Collider Physics (Hadron13), Mumbai, India, January 1999.

3. J. Dainton, "The Structure of Hadronic Physics", Max Born Lecture, Annual meeting of the German Physical Society, Heidelberg, Germany, March 1999.

4. T. McMahon, "Studies of real and virtual photon structure at HERA", 34th Rencontres de Moriond: QCD and Hadronic Interactions, Les Arcs, France, March 1999.

5. B. Cox, "High t diffraction at HERA", 7th International Workshop on Deep-Inelastic Scattering and QCD (DIS99), Zeuthen, Germany, April 1999.

6. P. Newman, "H1 Measurements of Open b Production", 7th International Workshop on Deep-Inelastic Scattering and QCD (DIS99), Zeuthen, Germany, April 1999.

7. D. Kant, "Fragmentation functions and rapidity spectra in the Breit frame at H1", 7th International Workshop on Deep-Inelastic Scattering and QCD (DIS99), Zeuthen, Germany, April 1999.

8. B. Cox, "High t Diffraction", Institute of Physics Conference, Salford, April 1999.

9. B. Waugh, "Elastic/Diffractive Vector Meson Production in Photoproduction", International Conference on the Structure and Interactions of the Photon (PHOTON99), Freiburg, Germany, May 1999.

10. P. Thompson, "Production of D^* mesons in deep-inelastic diffractive interactions at HERA", International Conference on the Structure and Interactions of the Photon (PHOTON99), Freiburg, Germany, May 1999.

11. T. Greenshaw, "Forward Jet and Hadron Production at Low x and Q^2", Ringberg HERA Phenomenology Workshop, Bavaria, Germany, May 1999.

12. J. Dainton, "Low x Physics", Frontiers of Matter (Rencontres de Blois), Gif-sur-Yvette, France, July 1999.

13. P. Newman, "Introductory Talk on Low-x and Diffractive Physics", UK Phenomenology Workshop on Collider Physics, Durham, UK, September 1999.

14. B. Cox, "Summary Talk on Low-x and Diffractive Physics", UK Phenomenology Workshop on Collider Physics, Durham, UK, September 1999.

15. J. Dainton, "Electron-Proton Physics at HERA - Beyond the Beginning", International Workshop on Symmetry and Spin (PRAHA-SPIN '99), Prague, Czech Republic, September 1999.

16. J. Dainton, "Low x Physics", International Workshop on Symmetry and Spin (PRAHA-SPIN '99), Prague, Czech Republic, September 1999.

17. D. Milstead, "Fragmentation and Power Corrections", XXIX International Symposium on Multiparticle Dynamics (ISMD99), Rhode Island, USA, Aug 1999.

18. A. Mehta, "Latest Results from HERA", 7th International Symposium on Particles, Strings and Cosmology (PASCOS99), Lake Tahoe, USA, December 1999.

9 H1 Conference Submissions 1999

The following papers were submitted by the H1 collaboration to the International Europhysics Conference on High Energy Physics (EPS 99), Tampere, Finland and the International Symposium on Lepton and Photon Interactions at High Energies (LP99), Stanford, USA.

1. EPS99 Abstract 157s, "Search for events with an isolated high energy lepton and missing transverse momentum at HERA"

2. EPS99 Abstract 157u, "Test of the Standard Model in high E_T jet production at HERA"

3. EPS99 Abstract 157c, "A Search for Leptoquark Bosons and Lepton Flavor Violation in Positron-Proton Collisions at HERA"

4. EPS99 Abstract 157f, "A Search for Contact Interactions in Neutral Current Scattering at HERA"

5. EPS99 Abstract 157ai, "Measurement of Neutral and Charged Current Cross-Sections in Positron-Proton Collisions at Large Momentum Transfer at HERA"

6. EPS99 Abstract 157b, "Measurement of the Neutral and Charged Current Cross Sections in Electron-Proton Collisions at High Q^2 at HERA"

7. EPS99 Abstract 157p, "Measurement of D^* Meson Cross Sections at HERA and Determination of the Gluon Density in the Proton using NLO QCD"

8. EPS99 Abstract 157r, "Measurement of Dijet Cross-Sections at Low Q^2 in ep Collisions and the Extraction of an Effective Parton Density for the Virtual Photon"

9. EPS99 Abstract 157j, "Study of the photon remnant in resolved photoproduction and low Q^2 processes at HERA"

10. EPS99 Abstract 157ad, "Dijet Cross Sections in Photoproduction and Determination of the Gluon Density in the Photon"

11. EPS99 Abstract 157g, "Test of QCD Dynamics at Small Parton Momenta x at HERA"

12. EPS99 Abstract 157, "Determination of the Strong Coupling Constant from Inclusive Jet Cross Sections"

13. EPS99 Abstract 157, "Measurement of Differential Jet Production in Deep-Inelastic Scattering at High Q^2 at HERA"

14. EPS99 Abstract 157 "Study of Three-Jet Production in Deep-Inelastic Positron Proton Collisions at HERA"

15. EPS99 Abstract 157x, "Measurement of Internal Jet Structure in Dijet Production in Deep-Inelastic Scattering at HERA"

16. EPS99 Abstract 157ae, "Diffractive dijet electroproduction at HERA"

17. EPS99 Abstract 157m, "Measurement of Leading Proton and Neutron Production in Deep Inelastic Scattering at HERA"

18. EPS99 Abstract 157ag, "Measurement of the production of D^* mesons in deep-inelastic diffractive interactions at HERA"

19. EPS99 Abstract 157o, "Charmonium Production in Deep Inelastic Scattering at HERA"

20. EPS99 Abstract 157aj, "Inelastic Photoproduction of J/ψ and $\psi(2S)$"

21. EPS99 Abstract 157n, "Proton Dissociative and Elastic Electroproduction of ρ^0 Mesons at HERA"

22. EPS99 Abstract 157k, "A study of event shape variables in deep-inelastic ep scattering at HERA"

23. EPS99 Abstract 157l, "Transverse energy flow in deep-inelastic ep Scattering at HERA"

24. EPS99 Abstract 157h, "A study of inclusive identified charged particle production in deep-inelastic scattering at HERA"

25. LP99 only, "W Production in e+-p collisions at HERA"

References

[1] 'The HERA Luminosity Upgrade', ed. U. Schneekloth, *DESY-HERA* **98-05** (1998).

[2] H1 Collaboration, *DESY* **99-107**, accepted by *Eur. Phys. J.*

[3] H1 Collab., 'Measurement of Neutral and Charged Current Cross-Sections in Electron-Proton Collisions at Large Momentum Transfer at HERA', paper 157b contributed to EPS99, Tampere, Finland, 1999.

[4] CDF Collaboration, F. Abe et al., *Phys. Rev. Lett.* **75** (1995) 11.
DØ Collaboration, B. Abbott et al., *Phys. Rev. Lett.* **80** (1998) 3008.
ALEPH Collaboration, R. Barate et al., *Phys. Lett.* **B422** (1998) 384.
DELPHI Collaboration, P. Abreu et al., *Eur. Phys. J.* **C2** (1998) 581.
L3 Collaboration, M. Acciarri et al., *Phys. Lett.* **B413** (1997) 176.
OPAL Collaboration, K. Ackerstaff et al., *Eur. Phys. J.* **C1** (1998) 395.

[5] H. Fritzsch, D. Holtmannspötter, *Phys. Lett.* **B457** (1999) 186.

[6] T. Kon, T. Matsushita, T. Kobayashi, *Mod. Phys. Lett.* **A12** (1997) 3143.

[7] H1 Collaboration, C. Adloff et al., *Eur. Phys. J.* **C5** (1998) 575.

[8] H1 Collaboration, 'W production in $e^{\pm}p$ collisions at HERA', Paper prepared for Lepton-Photon '99, Stanford, USA, 1999.

[9] H1 Collaboration, C.Adloff et al., *Z.Phys.* **C74** (1997) 221.

[10] J. Collins, *Phys. Rev.* **D57** (1998) 3051.

[11] G. Ingelman, P. Schlein, *Phys. Lett.* **B152** (1985) 256.

[12] L. Alvero, J. Collins and J. Whitmore, *Phys. Rev.* **D59** (1999) 074022.

[13] H1 Collaboration, 'Diffractive dijet electroproduction at HERA', paper 157ae contributed to EPS99, Tampere, Finland, 1999

[14] J. Bartles, H. Lotter, M. Wüsthoff, *Phys. Lett.* **B379** (1996) 239.
J. Bartles, C. Ewerz, H. Lotter, M. Wüsthoff, *Phys. Lett.* **B386** (1996) 389.

[15] H1 Collaboration, 'Measurement of the production of D^* mesons in deep-inelastic diffractive interactions at HERA', Paper 157ag contributed to EPS99, Tampere, Finland, 1999.
P. Thompson, 'Open Charm Production in Inclusive and Diffractive Deep-Inelastic Scattering at HERA', Ph.D. thesis (University of Birmingham), 1999.

[16] H1 Collaboration, C. Adloff et al., *Eur. Phys. J.* **C10** (1999) 373.

[17] H1 Collaboration, C. Adloff et al., *DESY* **99-010**, to appear in *Eur.Phys.J.*

[18] H1 Collaboration, 'Diffractive J/ψ Photoproduction', Paper 157o contributed to EPS99, Tampere, Finland, 1999.

[19] L. Frankfurt, W. Koepf, M. Strikman, *Phys. Rev.* **D54** (1996), 319.
L. Frankfurt, W. Koepf, M. Strikman, *Phys. Rev.* **D57** (1998), 512.

[20] H1 Collaboration, C. Adloff et al., *Phys. Lett.* **B467** (1999) 156.

[21] H1 Collaboration, 'A study of inclusive identified charged particle production in deep-inelastic scattering at HERA', Paper 157h contributed to EPS99, Tampere, Finland, 1999.

[22] P. Dixon, D. Kant and G. Thompson, *J. Phys. G* **Vol. 25 Num. 7** (1999) 1453.

[23] K.T. Donovan, D. Kant and G. Thompson, *Journ. Phys. G* **Vol. 25 Num. 7** (1999) 1448.

[24] D. Kant, *Nucl. Phys. B (Proc. Suppl.)* **71** (1999) 31.

[25] R.K. Griffiths, 'The First measure of Relative Partonic Contributions in DIS at HERA using an Average Hadronic Charge', Ph.D thesis, University of London, 1998.

[26] D. Graudenz, CERN TH/96-52, CERN TH/96-155 (hep-ph/9606460), CERN TH/96-187 (hep-ph/9610287).

[27] K.T. Donovan, 'Hadronic Fragmentation Studies in ep Scattering at HERA', Ph.D thesis, University of London, 1998.

[28] W. Ochs, Proceedings of the Ringberg Workshop "New Trends in HERA Physics", Tegernsee, Germany, 25-30 May 1997 hep/ph/9709248.

[29] R.-D. Appuhn et al., The electronics of the H1 lead/scintillating-fibre calorimeters, *Nucl. Instr. and Meth.* **A426** (1999) 518.

[30] H1 Collaboration, "Proposal for an Upgrade of the H1 Forward Track Detector for HERA 2000", DESY PRC proposal **PRC 98-06**, 1998.

[31] H1 Collaboration, "A fast Track Trigger with High Resolution for H1" and "Addendum", DESY PRC Proposals **PRC 99-06** and **PRC 99-07**, 1999.